A Space Optimization Method for Time-Reversal Super-Focusing

Jens Rautenberg, Dirk Olszewski, Bernd Henning

University of Paderborn, Institute for Electrical Engineering and Information Technology, Electrical Measurement Techniques, Warburger Str. 100, 33098 Paderborn, Germany
E-Mail: Rautenberg@emt.uni-paderborn.de

Abstract

The appliance of time-reversal acoustics to classical transducer design, medical, technical or audible range applications brings forward new ideas whenever we need both, focusing acoustical energy in time and space. Unfortunately, the spatiotemporal focusing is limited through the amount of applied transducer elements as well as the ergodicity and randomness of the cavity [1]. This paper will show how the simulated annealing technique, a multi-objective optimization algorithm [2], is used to increase the narrowness of the refocused spot by breaking up randomness for the benefit of ergodicity in a predetermined cavity.

Theory

Binary pseudo-random sequences that are generated by a *m*-stage shift register with linear feedback [3], ideally have an autocorrelation function (ACF, ϕ) with $\phi(\tau=0)=2^m-1$ and $\phi(\tau\neq 0)=-1$. If one feedback is changed in such a system, these properties could change completely. Figure 1 shows the ACFs of two sequences generated with the polynomials $g_1(x)=x^5+x^2+1$ and $g_2(x)=x^5+x^3+x^2+1$. One of the ACFs indicates ambiguities in the pseudo-random sequence.

In an acoustic cavity (Figure 1) a sound wave propagates on different paths and reflects on many boundaries (feedback). In linear time-invariant time-reversal acoustics the multiple-scattering medium can be interpreted as M matched filters for the M retransmitted signals $h_{i,m}(-t)$ which superpose to the response $y_i(t) = \phi_{\mathrm{hh},i}(t)$ at the N desired focus points r_i (Equation 1, [1]). Thus, good ACF properties at different focus points r_i suggest good time-reversal focusing capabilities. Any reciprocity error $n_{i,m}(t)$ during retransmission or back propagation will result in additional background noise or in a less ratio of the ACF maximum to the maxima of every possible spatial cross correlation function (CCF).

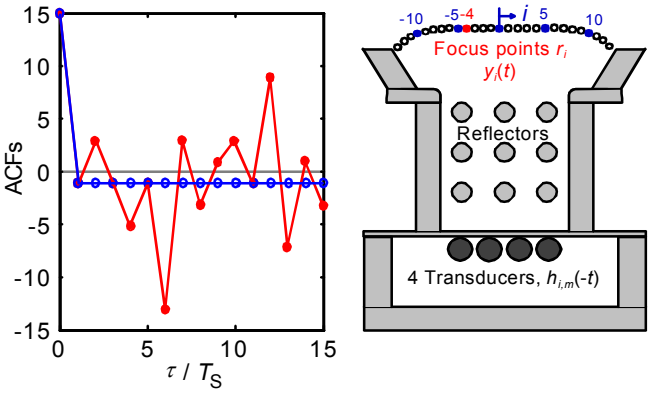

Figure 1: ACFs (left) of an ideal pseudo-random sequence (blue) and another binary sequence of the same length (red) – the acoustic cavity to be optimized (right)

With this, ambiguities in time-reversal focusing or matched filter beam forming [4] can be minimized by maximizing the uniqueness u of the pulse responses:

$$y_i(t)=\sum_{m=1}^{M} h_{i,m}(t)*h_{i,m}(-t)+\sum_{m=1}^{M} h_{i,m}(t)*n_{i,m}(t) \qquad (1)$$

$$u_i=\frac{\max\left(\left|\mathrm{ACF}_i\right|\right)}{\frac{1}{N-1}\sum_{j=1,j\neq i}^{N}\max\left(\left|\mathrm{CCF}_{i,j}\right|\right)} \qquad (2)$$

One selected ACF and the N-1 CCFs for the cavity are shown in Figure 3. The pulse after time-reversal cannot be more distinctive than the superposition of these functions.

In order to meet the abovementioned requirements, the positions of the cylindrical reflectors inside the acoustic cavity and therewith the paths of sound propagation are recombined within an inhomogeneous simulated annealing algorithm:

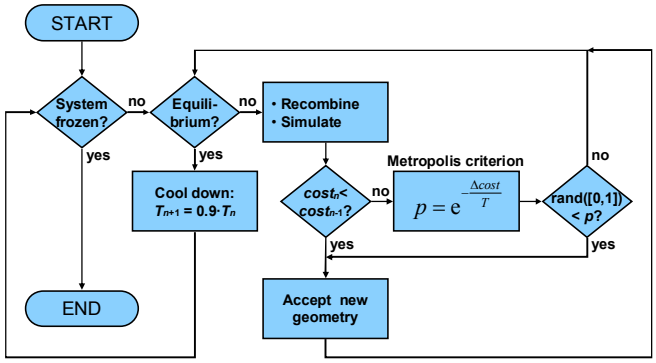

Figure 2: Inhomogeneous simulated annealing algorithm

Starting with an initial arrangement a new combination is accepted if it is better than the old one or if it fulfils the Metropolis criterion [2]. The latter case guarantees that the algorithm does not concentrate on local optima. With high temperature T the probability p of acceptance for worse

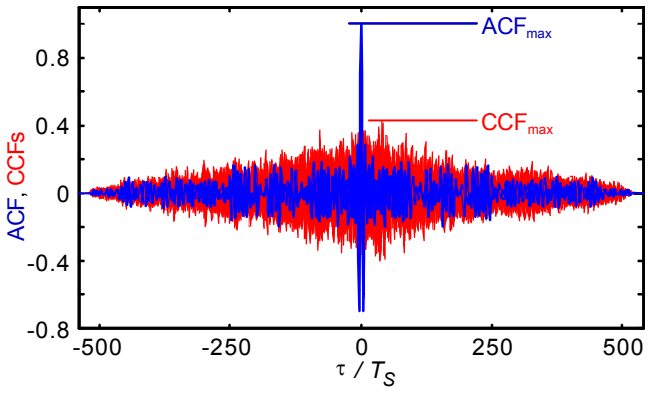

Figure 3: ACF of pulse response at one selected focus point (blue) and all CCFs with pulse responses at other focus points of interest (red)

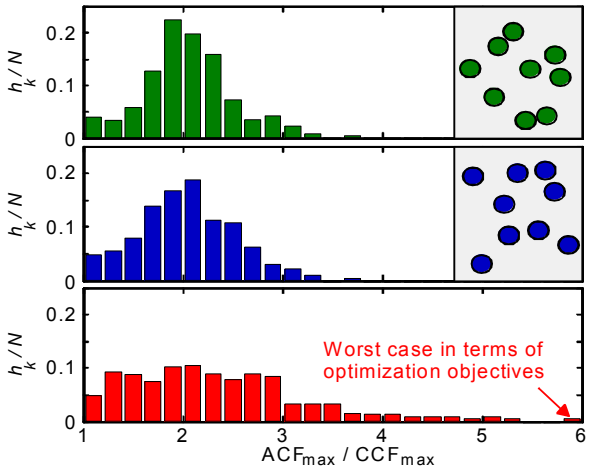

Figure 4: Histograms of ACF/CCF-ratios – best (green), coincidental (blue), worst arrangement of the reflectors (red)

solutions is also high. After q simulation steps the process is supposed to be in its equilibrium. Then the temperature and therewith the acceptance probability is decreased.

The simulation results are valued at the uniformity of u_i and the uniform distribution of the signal energies $h_{i,\mathrm{eff}}$, each determined by the standard deviations σ. Therewith every point of interest should be focusable with similar quality.

$$cost_1 = \frac{\sigma(u_i)}{1+\sigma(u_i)} = \sqrt{\frac{1}{N}\sum_{i=1}^{N}(u_i-\bar{u})}\left(\bar{u}+\sqrt{\frac{1}{N}\sum_{i=1}^{N}(u_i-\bar{u})}\right)^{-1} \quad (3)$$

$$cost_2 = \frac{\sigma(h_{i,\mathrm{eff}})}{1+\sigma(h_{i,\mathrm{eff}})} \quad (4)$$

In analogy to the molecules of a molten bath, the reflectors solidify with decreasing temperature so that the result should be a well-regulated system in terms of the preset objectives.

Results

Figure 4 shows the relative frequency of occurrence h_k of the ACF/CCF-ratios that are used for calculation of $cost_1$. There are only small distinctions in both the mean values and the standard deviations of the optimized ($cost_1$=0.157) and the coincidental arrangements ($cost_1$=0.167). The worst arrangement ($cost_1$=0.269) has a higher standard deviation. The ratios up to 6 indicate a well-suited solution if only some selected points are to focus on, but there will be no flexibility concerning variable and uniform directivity patterns.

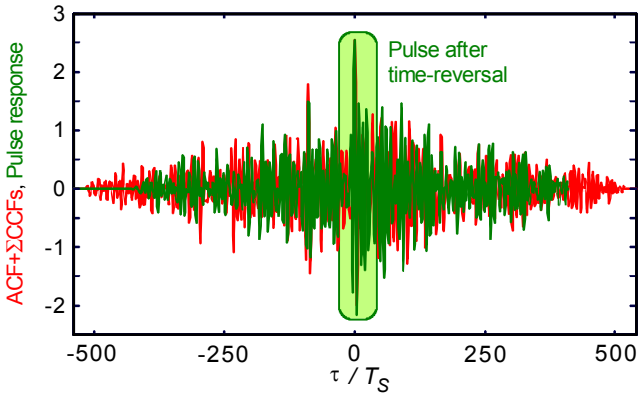

Figure 5: Temporal focusing – superposition of one selected ACF with all possible CCFs (red) and scaled pulse response after time-reversal (green)

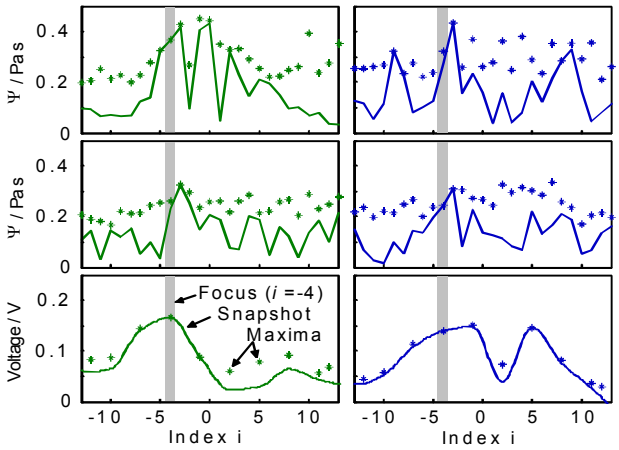

Figure 6: Spatial focusing – best (left) and coincidental system (right) – single channel (top) and four channel simulation (middle), measured voltages of the experiment (bottom)

The response after single channel time-reversed excitation is almost the superposition of the ACF and all CCFs (Figure 5) such as described in the theory. This temporal focusing was only observed with the optimized geometry.

The spatial focusing is observable in the velocity potential Ψ of both the optimized and coincidental system but the snapshots of the directivity patterns impressively show the desired suppression of side lobes in the optimized configuration (Figure 6). Noteworthy is the fact that a four channel excitation did not significantly increase the directivity.

An important step of simulation is the validation. Therefore the spatial focusing with single channel excitation was examined with a 40 kHz airborne experiment. As the relative bandwidth of the transducers is only at about 5%, the pulse responses are longer than those in simulation. With this the matched filter beam forming is much better in general but the side lobe suppression is also best with the optimized arrangement (Figure 6, bottom).

Conclusion

Simulations have shown that it is possible to improve both temporal and spatial focusing by appliance of the simulated annealing algorithm. The temporal compression in the considered example is as good as predicted. Furthermore it has been experimentally shown that minimization of the cost functions results in a good suppression of undesired side lobes or spatial ambiguities. With this the door is open for further developments in many application areas.

References

[1] Fink, M.: Acoustic Time-Reversal Mirrors. Topics in applied physics 84 (2002), 17-43

[2] Hopperstad, J. F.: Optimization of sparse arrays by an improved simulated annealing algorithm. Proc. Int. Workshop on Sampling Theory and Applications (Loen, Norway 1999), 91-95

[3] Proakis, J. G.: Digital Communications. McGRAW-HILL, New York, 1995

[4] Jensen, F. B.: Computational Ocean Acoustics. AIP Press, New York, 1993